Hindawi Publishing Corporation
Evidence-Based Complementary and Alternative Medicine
Volume 2016, Article ID 2635483, 21 pages
http://dx.doi.org/10.1155/2016/2635483

*Research Article*

# iTRAQ-Based Proteomic Analysis of Ginsenoside $F_2$ on Human Gastric Carcinoma Cells SGC7901

**Qian Mao,[1] Pin-Hu Zhang,[2] Jie Yang,[3] Jin-Di Xu,[1] Ming Kong,[1] Hong Shen,[1] He Zhu,[1] Min Bai,[1] Li Zhou,[1] Guang-Fu Li,[4] Qiang Wang,[3] and Song-Lin Li[1]**

[1]*Department of Pharmaceutical Analysis & Metabolomics, Affiliated Hospital of Integrated Traditional Chinese and Western Medicine, Nanjing University of Chinese Medicine, Nanjing 210028, China*
[2]*Jiangsu Center for New Drug Screening & National New Drug Screening Laboratory, China Pharmaceutical University, Nanjing 210009, China*
[3]*Department of Chinese Medicines Analysis, China Pharmaceutical University, Nanjing 210009, China*
[4]*Department of Surgery, The Medical University of South Carolina, Charleston, SC 29466, USA*

Correspondence should be addressed to Qiang Wang; qwang49@126.com and Song-Lin Li; songlinli64@126.com

Received 12 May 2016; Revised 4 August 2016; Accepted 25 August 2016

Academic Editor: Isabel Andújar



Ginsenoside $F_2$ ($F_2$), a protopanaxdiol type of saponin, was reported to inhibit human gastric cancer cells SGC7901. To better understand the molecular mechanisms of $F_2$, an iTRAQ-based proteomics approach was applied to define protein expression profiles in SGC7901 cells in response to lower dose (20 $\mu$M) and shorter duration (12 hour) of $F_2$ treatment, compared with previous study. 205 proteins were screened in terms of the change in their expression level which met our predefined criteria. Further bioinformatics and experiments demonstrated that $F_2$ treatment downregulated PRR5 and RPS15 and upregulated RPL26, which are implicated in ribosomal protein-p53 signaling pathway. $F_2$ also inhibited CISD2, Bcl-xl, and NLRX1, which are associated with autophagic pathway. Furthermore, it was demonstrated that $F_2$ treatment increased Atg5, Atg7, Atg10, and PUMA, the critical downstream effectors of ribosomal protein-p53 signaling pathway, and Beclin-1, UVRAG, and AMBRA-1, the important molecules in Bcl-xl/Beclin-1 pathway. The 6 differentially abundant proteins, PRR5, CISD2, Bcl-xl, NLRX1, RPS15, and RPL26, were confirmed by western blot. Taken together, ribosomal protein-p53 signaling pathway and Bcl-xl/Beclin-1 pathway might be the most significantly regulated biological process by $F_2$ treatment in SGC7901 cells, which provided valuable insights into the deep understanding of the molecular mechanisms of $F_2$ for gastric cancer treatment.

## 1. Introduction

Gastric cancer is the fifth most common cancer and the third leading cause of cancer-related death worldwide. Annually it results in approximately 700,000 deaths [1]. Currently, chemotherapy has proved to decrease the rate of recurrence and improve overall survival; however, the drug resistance and serious toxic side effects largely reduce therapeutic efficacy and quality of life in patients [2, 3]. In recent years, compounds of natural products have caught wide attention due to their promising anticancer effects and minimal side effects [4–7]. Therefore, it is very necessary to develop new optimal anticancer agent from natural resource [3].

Ginsenosides, the major bioactive constituents in ginseng, have been demonstrated to exert potential anticancer ability [4, 5]. Exploration of ginsenoside as a new anticarcinogenic agent is of much interest [4–7]. Structural-function studies showed that the increased antitumor effect is implicated with the decrease of its sugar number [5]. Sugar moiety at C-6 significantly reduces the anticancer activities of ginsenosides. Ginsenoside $F_2$ (see structure in Figure 1), a protopanaxdiol type ginsenoside with one sugar molecular at C-3 and one sugar molecule at C-20, has been shown to be potent in inhibiting tumorigenesis in several different cancers including gastric tumor and glioblastoma multiforme [6, 7]. Recently, our *in vitro* and *in vivo* studies demonstrated that

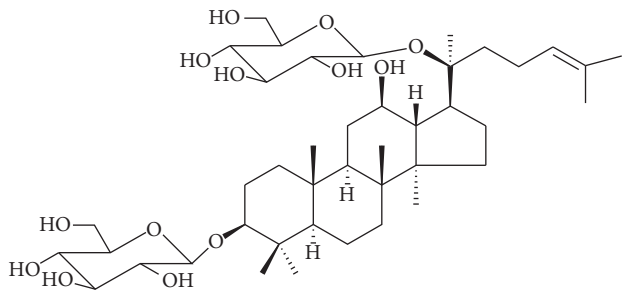

Figure 1: Structure of ginsenoside $F_2$.

ginsenoside $F_2$ possesses anticancer effects in human gastric carcinoma cells SGC7901 [6]. However, the involved exact mechanisms of ginsenoside $F_2$ on SGC7901 cancer cells at proteome level have not been systemically investigated.

Advancements in the field of proteomics have made it possible to accurately monitor and quantitatively detect the changes of protein expression in response to drug treatment. The achieved data provide valuable insights into the molecular mechanisms of disease and help to identify therapeutic targets [8]. Isobaric tag for relative and absolute quantification (iTRAQ) is a robust mass spectrometry technique that allows quantitative comparison of protein abundance by measuring peak intensities of reporter ions released from iTRAQ-tagged peptides by fragmentation. iTRAQ with multiplexing capability up to eight distinct samples in a single experiment and relatively higher sensitivity has gained significant interest in the field of quantitative proteomics. In the present study, SGC7901 cells treated by lower dose and a shorter duration than that in previous report were analyzed by iTRAQ-based proteomics integrated with bioinformatics using Gene Ontology (GO), Kyoto Encyclopedia of Genes and Genomes (KEGG), and Cluster of Orthologous Groups (COG) of proteins database. And network analysis was applied to identify critical molecules which are involved in anticancer mechanisms of ginsenoside $F_2$ in gastric SGC7901 cells. General molecular biological techniques such as western blot were utilized for validation.

## 2. Materials and Methods

*2.1. Reagents and Antibodies.* Ginsenoside $F_2$ was isolated previously from leaves of *Panax ginseng* by a series of chromatographic procedures [9]. Ginsenoside $F_2$ has a molecular mass of 784 Da and was isolated with 98% purity. Primary antibodies of PRR5, CISD2, Bcl-2L, NLRX1, RPS15, RPL26, p53, PUMA, Beclin-1, UVRAG, AMBRA-1, mTOR, LC3-II, LC3-I, and $\beta$-actin together with all secondary antibodies were purchased from Cell Signaling Technology (Danvers, MA, USA). The Atg5, Atg7, and Atg10 antibodies were obtained from Santa Cruz Biotechnology (Santa Cruz, CA, USA).

*2.2. Cell Culture and Treatment.* SGC7901 cells were purchased from American Type Culture Collection and maintained in Dulbecco's modified Eagle's medium (Hyclone) supplemented with 10% fetal bovine serum (FBS), 100 $\mu$g/mL streptomycin, and 100 $\mu$g/mL penicillin and grown at 37°C in 5% carbon dioxide.

*2.3. Protein Preparation.* In one of our recent reports [6], we have shown that the $IC_{50}$ of ginsenoside $F_2$ is in <50 $\mu$M in 24 hours. In order to characterize ginsenoside $F_2$-related mechanism it is imperative to use samples that are at the early stages of ginsenoside $F_2$ treatment. So, a lower dose than the $IC_{50}$ (20 $\mu$M) and a shorter duration (12 hours in the study) were chosen in the study. The treated (20 $\mu$M) and untreated SGC7901 cells were suspended in the lysis buffer and sonicated in ice. The proteins were reduced with 10 $\mu$M DTT (final concentration) at 56°C for 1 h and then alkylated by 55 mM iodoacetamide (IAM) (final concentration) in the darkroom for 1 h. The reduced and alkylated protein mixtures were precipitated by adding 4x volume of chilled acetone at −20°C overnight. After centrifugation at 4°C, 30 000 ×g, the pellet was dissolved in 0.5 M triethylammonium bicarbonate (TEAB) (Applied Biosystems, Milan, Italy) and sonicated in ice. After centrifuging at 30000 ×g at 4°C, the supernatants were collected, and the total protein concentration was determined using a Bradford protein assay kit (BioRad, Hercules, CA, USA). The proteins in the supernatant were kept at −80°C for further analysis.

*2.4. iTRAQ Labeling and SCX Fractionation.* Total protein (100 $\mu$g) was taken out of each sample solution and then the protein was digested with Trypsin Gold (Promega, Madison, WI, USA) with the ratio of protein : trypsin = 30 : 1 at 37°C for 16 hours. iTRAQ labeling was performed according to the iTRAQ Reagents-8plex labeling manual (AB SCIEX, Madrid, Spain). Briefly, one unit of iTRAQ reagent was thawed and reconstituted in 24 $\mu$L isopropanol. iTRAQ labels 113 were used to label control sample separately, and 115 and 117 were used to label twice $F_2$-treated samples for duplicated experiment. The peptides were labeled with the isobaric tags, incubated at room temperature for 2 h. The labeled peptide mixtures were then pooled and dried by vacuum centrifugation.

The mixed peptides were fractionated by strong cation exchange (SCX) chromatography on a LC-20AB HPLC Pump system (Shimadzu, Kyoto, Japan). The iTRAQ labeled peptide mixtures were reconstituted with 4 mL buffer A (25 mM $NaH_2PO_4$ in 25% acetonitrile, pH 2.7) and loaded onto a 4.6 ×

250 mm Ul tremex SCX column containing 5 $\mu$m particles (Phenomenex). The peptides were eluted at a flow rate of 1 mL/min with a gradient of buffer A for 10 min, 5–60% buffer B (25 mM $NaH_2PO_4$, 1 M KCl in 25% acetonitrile, pH 2.7) for 27 min, and 60–100% buffer B for 1 min. The system was then maintained at 100% buffer B for 1 min before equilibrating with buffer A for 10 min prior to the next injection. Elution was monitored by measuring the absorbance at 214 nm, and fractions were collected at 1-minute intervals. The eluted peptides were pooled into 20 fractions, desalted with a Strata X C18 column (Phenomenex), and vacuum-dried. The cleaned fractions were then lyophilized again and stored at −20°C until analyzed by mass spectrometry.

*2.5. LC-ESI-MS/MS Analysis Based on Q EXACTIVE.* Each fraction was resuspended in buffer A (2% acetonitrile, 0.1% FA) and centrifuged at 20 000 ×g for 10 min. In each fraction, the final concentration of peptide was about 0.5 $\mu$g/$\mu$L. 10 $\mu$L supernatant was loaded on a LC-20AD nano-HPLC (Shimadzu, Kyoto, Japan) by the autosampler onto a 2 cm C18 trap column. Then, the peptides were eluted onto a 10 cm analytical C18 column (inner diameter 75 $\mu$m) packed in-house. The samples were loaded at 8 $\mu$L/min for 4 min; then the 44 min gradient was run at 300 nL/min starting from 2 to 35% B (98% acetonitrile, 0.1% FA), followed by 2-minute linear gradient to 80%, maintenance at 80% B for 4 min. Initial chromatographic conditions were restored in 1 min.

Data acquisition was performed with tandem mass spectrometry (MS/MS) in a Q EXACTIVE (Thermo Fisher Scientific, San Jose, CA) coupled online to the HPLC. Intact peptides were detected in the Orbitrap at a resolution of 70 000. Peptides were selected for MS/MS using high-energy collision dissociation (HCD) operating mode with a normalized collision energy setting of 27.0; ion fragments were detected in the Orbitrap at a resolution of 17500. In the octopole collision cell, the ten most intense peptide ions (charge states ≥ 2) were sequentially isolated to a maximum target value of $5 \times 10^5$ by pAGC and fragmented HCD. A data-dependent procedure that alternated between one MS scan and 15 MS/MS scans was applied for the 15 most abundant precursor ions above a threshold ion count of 20000 in the MS survey scan with a following Dynamic Exclusion duration of 15 s. The electrospray voltage applied was 1.6 kV. Automatic gain control (AGC) was used to optimize the spectra generated by the Orbitrap. A sweeping collision energy setting of 35 ± 5 eV was applied to all precursor ions for collision-induced dissociation. The AGC target for full MS was $3e^6$ and $1e^5$ for $MS^2$. For MS scans, the $m/z$ scan range was 350 to 2000 Da. For $MS^2$ scans, the $m/z$ scan range was 100–1800 Da. The iTRAQ experiments were performed as three technical replicates to gather reliable quantitative information.

*2.6. Data Analysis.* Raw data files acquired from the Orbitrap were converted into MGF files using Proteome Discoverer 1.2 (PD 1.2, Thermo) [5600 msconverter] and the MGF files were searched. Protein identifications were performed by using Mascot search engine (Matrix Science, London, UK; version 2.3.02) against database containing 143397 sequences.

For protein identification and quantification, a peptide mass tolerance of 20 ppm was allowed for intact peptide masses and 0.05 Da for fragmented ions, with allowance for one missed cleavage in the trypsin digests. Carbamidomethylation of cysteine was considered a fixed modification, and the conversion of *N*-terminal glutamine to pyroglutamic acid and methionine oxidation were considered variable modifications. All identified peptides had an ion score above the Mascot peptide identity threshold, and a protein was considered identified if at least one such unique peptide match was apparent for the protein. To reduce the probability of false peptide identification, only peptides at the 95% confidence interval by a Mascot probability analysis greater than "identity" were counted as identified. The quantitative protein ratios were weighted and normalized by the median ratio in Mascot. We set a 1.2-fold change as the threshold and a $p$ value must be below 0.05 to identify significant changes.

*2.7. Function Method Description.* Functional annotations of the proteins were conducted using Blast2 GO program against the nonredundant protein database (NR; NCBI). The KEGG database (http://www.genome.jp/kegg/) and the COG database (http://www.ncbi.nlm.nih.gov/COG/) were used to classify and group these identified proteins.

GO is an international standardization of gene function classification system. It provides a set of dynamic updating controlled vocabulary to describe genes and gene products attributes in the organism. GO has 3 ontologies which can describe molecular function, cellular component, and biological process, respectively.

COG is the database for protein orthologous classification. Every protein in COG is supposed to derive from a same protein ancestor.

KEGG PATHWAY is a collection of manually drawn pathway maps representing our knowledge on the molecular interaction and reaction networks. Molecules are represented as nodes, and the biological relationship between two nodes is represented as an edge (line).

*2.8. Western Blot.* Western blot analyses were performed to confirm the presence of differentially expressed proteins. After the treatment of the indicated concentration of ginsenoside $F_2$ (10, 20, and 40 $\mu$M) for 12 h, cells were harvested, washed with cold PBS (pH 7.4), and lysed with ice-cold lysis buffer (50 $\mu$M Tris-HCl, 150 $\mu$M NaCl, 1 $\mu$M EGTA, 1 $\mu$M EDTA, 20 $\mu$M NaF, 100 $\mu$M $Na_3VO_4$, 1%NP40, 1 $\mu$M PMSF, 10 $\mu$g/mL aprotinin, and 10 $\mu$g/mL leupeptin, pH 7.4) for 30 min and centrifuged at 12 000 ×g for 30 min at 4°C. The protein concentration of the clear supernatant was quantified using Bio-Rad Protein Assay Kit.

Approximately 30 $\mu$g of protein was loaded into a 10–15% sodium dodecyl sulfate polyacrylamide gel electrophoresis (SDS–PAGE). Thereafter, proteins were electrophoretically transferred to nitrocellulose membrane and nonspecific sites were blocked with 5% skimmed milk in 1% Tween-20 (Sigma-Aldrich) in 20 $\mu$M TBS (pH 7.5) and reacted with a primary polyclonal antibody, PRR5, CISD2, Bcl-2L, NLRX1, RPS15, RPL26, p53, Atg5, Atg7, Atg10, LC3-II, LC3-I PUMA, Beclin-1, UVRAG, and mTOR and $\beta$-actin

for 4 h at room temperature. After washing with TBS three times (5 min each), the membrane was then incubated with alkaline phosphatase-conjugated goat anti-rabbit secondary antibody. The signal was observed and developed with Kodak film by exposure to enhanced chemiluminescence (ECL) plus western Blotting Detection Reagents (Amersham Biosciences, Piscataway, NJ, USA).

*2.9. Statistical Analysis.* For cell-based assay, experiments were performed in duplicate and three independent experiments were performed. Western blot analyses of differential protein expressions were validated on cell lysates from three biological replicates. Statistical significance was analyzed using Student's $t$-test or ANOVA test by using GraphPad Prism v4.0 software (GraphPad Software, San Diego, CA, USA). Statistical significance is expressed as $^{***}p < 0.001$; $^{**}p < 0.01$; $^{*}p < 0.05$.

## 3. Results

*3.1. Proteome Analysis.* Human gastric carcinoma cells (SGC7901) are treated with ginsenoside $F_2$ at a dose of 20 $\mu$M for 12 hours. The harvested proteins are used to perform iTRAQ for quantifying the difference of total 31853 peptides and 5411 proteins in SGC7901 cells with or without treatment. Finally, 205 proteins were screened out in terms of the change in their expression level which meet our predefined criteria of $p < 0.05$ with relative expression levels at least >1.2-fold (Table 1) or <0.83-fold (Table 2) (both 113/115 and 113/117) in ginsenoside $F_2$-treated group compared with the control group. The protein properties, including pI, molecular weight (MW), and number of residues were calculated by Mascot. The results are highly reproducible in two individual experiments.

*3.2. Classification of Differentially Expressed Proteins.* Firstly, screened proteins were functionally catalogued with GO and WEGO to three different groups (Figures 2 and 3(a)): biological process (BP), cellular component (CC), and molecular function (MF). As shown in Figure 2, the proteins are involved in BP including cellular process (13.44%), metabolic process (11.16%), single-organism process (10.36%), biological regulation (8.06%), and regulation of biological process (7.59%). The identified proteins separated according to CC include cell (19.40%), cell part (19.40%), organelle (16.68%), organelle part (12.46%), membrane (7.97%), and macromolecular complex (7.94%). MF of the proteins was classified and large groups were found to be binding (50.59%), catalytic activity (27.97%), enzyme regulator activity (3.94%), transporter activity (3.84%), and structural molecular activity (3.43%).

Further COG function classification revealed that post-translational modification, protein turnover, and ribosomal structure biogenesis were major function of the screened 205 proteins (Figure 3(b)). In each category of BP, CC, and MF, top twenty proteins which generated bigger difference in response to ginsenoside $F_2$ treatment are listed in Figure 4.

KEGG is a publicly available pathway database and could provide biologists excellent resources to attain a deeper understanding of biological mechanisms in response to different treatments. Protein analysis through KEGG indicated that 205 differentially expressed proteins were involved in 128 different pathways (data not shown). The connection degree between proteins is calculated by protein-protein interaction network analysis and the results are shown in Figure 5. Among these proteins, PRR5, RPS15, and RPL26 were found in ribosomal protein signaling pathway; CISD2, Bcl-xl, and NLRX1 were found in Beclin-1/Bcl-xL pathway. Therefore, PRR5, RPS15, RPL26, CISD2, Bcl-xl, and NLRX1 were selected for further validation and study in order to provide a comprehensive perspective for elucidating underlying molecular mechanisms of ginsenoside $F_2$.

*3.3. Western Blot Analysis*

*3.3.1. For Verification.* To validate the information obtained from the iTRAQ-based quantitative proteomics study and bioinformatics analysis, the screened proteins with strong response to ginsenoside $F_2$ treatment were further confirmed by western blot. As shown in Figure 6, ginsenoside $F_2$ significantly reduced protein expressions of PRR5, CISD2, Bcl-xl, NLRX1, and RPS15 ($p < 0.01$) and enhanced the expression of the RPL26 ($p < 0.01$) in SGC7901 cells in comparison with the treatment with vehicle control.

*3.3.2. For Determining the Expression of Apoptosis and Autophagic Proteins.* As shown in Figure 6, ginsenoside $F_2$ suppressed the expression of mTOR and upregulated the expression of p53 in a dose-dependent manner. Atg5, Atg7, Atg10, PUMA, Beclin-1, UVRAG, and AMBRA-1 are known to be modulated by p53 or Bcl-xl signaling, which may trigger apoptosis or autophagy. Therefore, we proceeded to check the expressions of Atg5, Atg7, Atg10, PUMA, Beclin-1, UVRAG, and AMBRA-1. As shown in Figure 7, ginsenoside $F_2$ upregulated the expressions of these proteins in a dose-dependent manner. LC3 is now widely used to monitor autophagy. During autophagy, the cytoplasmic form LC3-I is processed and recruited to phagophores, where LC3-II is generated by site-specific proteolysis and lipidation at the C-terminus. Thus, the amount of LC3-II positively correlates with the number of autophagosomes [10]. We examined the effect of $F_2$ on LC3 conversion in SGC7901 cells. Western blot analysis showed that $F_2$ treatment resulted in dose-dependent accumulation of LC3-II and reduction of LC3-I (Figure 7). The conversion of LC3-I to LC3-II suggested $F_2$ treatment induces autophagy.

In the present study, combination of iTRAQ-based proteomics method with bioinformatics was used to identify critical molecules in SGC7901 cancer cells in response to ginsenoside $F_2$ treatment. Ginsenoside $F_2$ generated significant change of protein profile in SGC7901 cells. Some of them have been demonstrated to participate in either apoptosis or autophagy responses, suggesting that the antitumor mechanisms of ginsenoside $F_2$ in SGC7901 cells are involved in both apoptosis and autophagy.

The current findings demonstrate that ginsenoside $F_2$ impacts distinct signaling pathways and induces broad change in the protein profile of SGC7901 cells. Overall, 205

Table 1: Differentially upregulated (>1.20-fold) proteins identified by iTRAQ in $F_2$ treated SGC7901 cells.

| Rank # | Accession | Gene symbol (GN) | Definition (description) | Score | Mass | Cov% | Ration | COG function-description |
|---|---|---|---|---|---|---|---|---|
| Up 1 | sp\|P07305-2 | H1F0 | Isoform 2 of histone H1.0 | 51 | 35582 | 13 | 2.11 | — |
| Up 2 | sp\|P20962 | PTMS | Parathymosin | 503 | 15782 | 23.5 | 1.32 | — |
| Up 3 | tr\|B8ZWD1 | DBI | Diazepam binding inhibitor, splice form 1A(2) | 121 | 15706 | 28.9 | 1.31 | Acyl-CoA-binding protein |
| Up 4 | sp\|Q16576 | RBBP7 | Histone-binding protein RBBP7 | 877 | 55737 | 24.5 | 1.25 | FOG: WD40 repeat |
| Up 5 | sp\|P46779-2 | RPL28 | Isoform 2 of 60S ribosomal protein L28 | 524 | 22107 | 27.6 | 1.35 | — |
| Up 6 | tr\|B2R514 | — | cDNA, FLJ92300, Homo sapiens COP9 subunit 6 (MOV34 homolog, 34 kD) (COPS6), mRNA | 74 | 39068 | 20.2 | 1.22 | Predicted metal-dependent protease of the PAD1/JAB1 superfamily |
| Up 7 | tr\|B3KY12 | — | cDNA FLJ46581 fis, clone THYMU3043200, highly similar to splicing factor 3A subunit 3 | 527 | 71859 | 22 | 1.24 | Splicing factor 3a, subunit 3 |
| Up 8 | sp\|Q71DI3 | HIST2H3A | Histone H3.2 | 617 | 19694 | 26.5 | 1.40 | Histones H3 and H4 |
| Up 9 | tr\|Q9P0H9 | RER1 | RER1 protein | 118 | 28927 | 22 | 1.26 | Golgi protein involved in Golgi-to-ER retrieval |
| Up 10 | tr\|A8K3Q9 | — | cDNA FLJ76611, highly similar to Homo sapiens ribosomal protein L14 (RPL14), mRNA | 781 | 35114 | 25.9 | 2.24 | Ribosomal protein L14E/L6E/L27E |
| Up 11 | sp\|Q9Y3A2 | UTP11L | Probable U3 small nucleolar RNA-associated protein 11 | 94 | 44174 | 21.7 | 1.30 | Uncharacterized conserved protein |
| Up 12 | tr\|F2Z388 | RPL35 | 60S ribosomal protein L35 | 99 | 15372 | 32.3 | 1.35 | Ribosomal protein L29 |
| Up 13 | sp\|Q9NZZ3 | CHMP5 | Charged multivesicular body protein 5 | 268 | 32218 | 21 | 1.42 | — |
| Up 14 | tr\|B2R4D8 | — | 60S ribosomal protein L27 | 398 | 23061 | 36 | 1.28 | Ribosomal protein L14E/L6E/L27E |
| Up 15 | tr\|M0QXF7 | C19orf10 | UPF0556 protein C19orf10 (fragment) | 265 | 11851 | 25 | 1.24 | — |
| Up 16 | tr\|D3DV26 | S100A10 | S100 calcium binding protein A10 (annexin II ligand, calpactin I, light polypeptide (P11)), isoform CRA_b (fragment) | 134 | 27935 | 8.3 | 1.21 | — |
| Up 17 | tr\|H7C2N1 | PTMA | Thymosin alpha-1 (fragment) | 117 | 18283 | 8.8 | 1.30 | — |
| Up 18 | tr\|G2XKQ0 | — | Sumo13 | 60 | 14938 | 11.9 | 1.22 | Ubiquitin-like protein (sentrin) |
| Up 19 | tr\|I3L1Y9 | FLYWCH2 | FLYWCH family member 2 | 99 | 19302 | 47.2 | 1.45 | — |
| Up 20 | tr\|M0R210 | RPS16 | 40S ribosomal protein S16 | 1105 | 19391 | 57.4 | 1.27 | Ribosomal protein S9 |
| Up 21 | sp\|O43715 | TRIAP1 | TP53-regulated inhibitor of apoptosis 1 | 82 | 12050 | 18.4 | 1.36 | — |
| Up 22 | sp\|P49207 | RPL34 | 60S ribosomal protein L34 | 187 | 18684 | 20.5 | 1.66 | Ribosomal protein L34E |
| Up 23 | sp\|Q92522 | H1FX | Histone H1x | 342 | 35250 | 25.4 | 1.33 | — |
| Up 24 | tr\|J3KRX5 | RPL17 | 60S ribosomal protein L17 (fragment) | 795 | 27382 | 38.5 | 1.26 | Ribosomal protein L22 |
| Up 25 | sp\|P02795 | MT2A | Metallothionein-2 | 104 | 9915 | 52.5 | 1.42 | — |
| Up 26 | tr\|Q6FIE5 | PHP14 | PHP14 protein | 72 | 17301 | 8.8 | 1.27 | — |
| Up 27 | tr\|A0PJ62 | RPL14 | RPL14 protein (fragment) | 536 | 21409 | 43.5 | 2.85 | Ribosomal protein L14E/L6E/L27E |
| Up 28 | tr\|G3XAA2 | MAP4K4 | Mitogen-activated protein kinase kinase kinase kinase 4 | 142 | 156989 | 2.7 | 1.24 | Serine/threonine protein kinase |

Table 1: Continued.

| Rank # | Accession | Gene symbol (GN) | Definition (description) | Score | Mass | Cov% | Ration | COG function-description |
|---|---|---|---|---|---|---|---|---|
| Up 29 | tr\|C9JNW5 | RPL24 | 60S ribosomal protein L24 | 666 | 24642 | 32 | 1.67 | Ribosomal protein L24E |
| Up 30 | sp\|Q13951 | CBFB | Core-binding factor subunit beta | 197 | 24461 | 18.1 | 1.20 | — |
| Up 31 | tr\|D3DUE6 | N-PAC | Cytokine-like nuclear factor n-pac, isoform CRA_c | 219 | 76728 | 14.5 | 1.24 | 3-Hydroxyisobutyrate dehydrogenase and related beta-hydroxy acid dehydrogenases |
| Up 32 | tr\|K7EKW4 | ISOC2 | Isochorismatase domain-containing protein 2, mitochondrial (fragment) | 130 | 21202 | 17.4 | 1.34 | Amidases related to nicotinamidase |
| Up 33 | sp\|Q9NQ55-2 | PPAN | Isoform 2 of Suppressor of SWI4 1 homolog | 73 | 63713 | 10.7 | 1.37 | — |
| Up 34 | tr\|B3KMF8 | — | cDNA FLJ10869 fis, clone NT2RP4001677 | 127 | 12398 | 27.7 | 1.28 | — |
| Up 35 | sp\|P62424 | RPL7A | 60S ribosomal protein L7a | 613 | 42316 | 27.1 | 1.78 | Ribosomal protein HS6-type (S12/L30/L7a) |
| Up 36 | tr\|B4E0X1 | — | Beta-2-microglobulin | 185 | 17093 | 13.1 | 1.25 | — |
| Up 37 | tr\|H0Y7A7 | CALM2 | Calmodulin (fragment) | 735 | 24209 | 30.5 | 1.26 | $Ca^{2+}$-binding protein (EF-Hand superfamily) |
| Up 38 | tr\|J3KTJ8 | RPL26 | 60S ribosomal protein L26 (fragment) | 363 | 15545 | 34 | 1.24 | Ribosomal protein L24 |
| Up 39 | tr\|B4DJM5 | — | cDNA FLJ61294, highly similar to keratin, type I cytoskeletal 17 | 326 | 21291 | 24.9 | 1.46 | — |
| Up 40 | sp\|Q9Y3C1 | NOP16 | Nucleolar protein 16 | 79 | 27925 | 20.8 | 1.24 | — |
| Up 41 | sp\|Q16543 | CDC37 | Hsp90 cochaperone Cdc37 | 384 | 57730 | 29.6 | 1.22 | — |
| Up 42 | sp\|P16401 | HIST1H1B | Histone H1.5 | 801 | 42644 | 17.3 | 2.38 | — |
| Up 43 | sp\|Q07866-3 | KLC1 | Isoform G of kinesin light chain 1 | 642 | 81828 | 23.9 | 1.24 | FOG: TPR repeat |
| Up 44 | tr\|B4DKJ4 | — | cDNA FLJ57738, highly similar to translationally controlled tumor protein | 344 | 19250 | 32.4 | 1.28 | — |

Table 2: Differentially downregulated (<0.83-fold) proteins identified by iTRAQ in $F_2$ treated SGC7901 cells.

| Rank # | Accession | Gene symbol (GN) | Definition (description) | Score | Mass | Cov% | Ration | COG function-description |
|---|---|---|---|---|---|---|---|---|
| Down 1 | tr\|F5H740 | VDAC3 | Voltage-dependent anion-selective channel protein 3 | 1114 | 39598 | 41.5 | 0.81 | — |
| Down 2 | sp\|Q9H845 | ACAD9 | Acyl-CoA dehydrogenase family member 9, mitochondrial | 311 | 81512 | 21.9 | 0.69 | Acyl-CoA dehydrogenases |
| Down 3 | sp\|Q969S9-2 | GFM2 | Isoform 2 of ribosome-releasing factor 2, mitochondrial | 153 | 94059 | 5.1 | 0.80 | Translation elongation factors (GTPases) |
| Down 4 | sp\|P35908 | KRT2 | Keratin, type II cytoskeletal 2 epidermal | 338 | 76630 | 18.2 | 0.67 | Myosin heavy chain |
| Down 5 | tr\|B7Z8A2 | — | cDNA FLJ51671, highly similar to prenylcysteine oxidase (EC 1.8.3.5) | 492 | 63740 | 23.8 | 0.83 | — |
| Down 6 | sp\|Q9Y512 | SAMM50 | Sorting and assembly machinery component 50 homolog | 170 | 59339 | 18.6 | 0.76 | Outer membrane protein/protective antigen OMA87 |
| Down 7 | sp\|Q6ZNW5 | GDPGP1 | GDP-D-glucose phosphorylase 1 | 118 | 45302 | 8.6 | 0.78 | — |
| Down 8 | sp\|P51970 | NDUFA8 | NADH dehydrogenase [ubiquinone] 1 alpha subcomplex subunit 8 | 72 | 25720 | 15.1 | 0.68 | — |
| Down 9 | tr\|B4DRW0 | — | cDNA FLJ58125, highly similar to copper-transporting ATPase 1 (EC 3.6.3.4) | 102 | 61873 | 6.1 | 0.78 | Cation transport ATPase |
| Down 10 | tr\|Q8NBW7 | KDELR1 | ER lumen protein retaining receptor | 51 | 20327 | 12.7 | 0.73 | ER lumen protein retaining receptor |
| Down 11 | tr\|B2R6F5 | — | cDNA, FLJ92928, highly similar to Homo sapiens retinitis pigmentosa 2 (X-linked recessive) (RP2), mRNA | 59 | 47451 | 2.3 | 0.82 | — |
| Down 12 | tr\|Q2VIN3 | — | RBM1 (fragment) | 1232 | 45756 | 26.8 | 0.81 | RNA-binding proteins (RRM domain) |
| Down 13 | sp\|P14174 | — | Macrophage migration inhibitory factor | 608 | 13856 | 17.4 | 0.71 | — |
| Down 14 | tr\|B2R6S4 | — | cDNA, FLJ93089, highly similar to Homo sapiens NCK adaptor protein 1 (NCK1), mRNA | 137 | 53755 | 18.3 | 0.83 | — |
| Down 15 | sp\|Q16822 | PCK2 | Phosphoenolpyruvate carboxykinase [GTP], mitochondrial | 1795 | 78784 | 41.6 | 0.74 | Phosphoenolpyruvate carboxykinase (GTP) |
| Down 16 | tr\|E9PM12 | TCIRG1 | V-type proton ATPase 116 kDa subunit a isoform 3 (fragment) | 63 | 25815 | 13.3 | 0.74 | Archaeal/vacuolar-type $H^+$-ATPase subunit I |
| Down 17 | sp\|Q2T9J0-2 | TYSND1 | Isoform 2 of peroxisomal leader peptide-processing protease | 96 | 43618 | 9.8 | 0.67 | — |
| Down 18 | tr\|J3KPX7 | PHB2 | Prohibitin-2 | 1543 | 39466 | 51.8 | 0.82 | Membrane protease subunits, stomatin/prohibitin homologs |
| Down 19 | tr\|Q8NCF7 | — | cDNA FLJ90278 fis, clone NT2RP1000325, highly similar to phosphate carrier protein, mitochondrial precursor | 517 | 48576 | 26.9 | 0.81 | — |
| Down 20 | tr\|B4E0R0 | — | cDNA FLJ54220, highly similar to Long-chain-fatty-acid-CoA ligase 1 (EC 6.2.1.3) | 100 | 88560 | 6.2 | 0.74 | Long-chain acyl-CoA synthetases (AMP-forming) |
| Down 21 | tr\|B3KRY3 | — | cDNA FLJ35079 fis, clone PLACE6005283, highly similar to lysosome-associated membrane glycoprotein 1 | 319 | 48851 | 11.1 | 0.79 | — |
| Down 22 | tr\|B3KU09 | — | cDNA FLJ39034 fis, clone NT2RP7008085, highly similar to Homo sapiens ring finger protein 123 (RNF123), mRNA | 110 | 166029 | 2.4 | 0.78 | — |
| Down 23 | sp\|Q9BVV7 | TIMM21 | Mitochondrial import inner membrane translocase subunit Tim21 | 86 | 35219 | 13.7 | 0.82 | — |

Table 2: Continued.

| Rank # | Accession | Gene symbol (GN) | Definition (description) | Score | Mass | Cov% | Ration | COG function-description |
|---|---|---|---|---|---|---|---|---|
| Down 24 | sp\|Q9UMY1 | NOL7 | Nucleolar protein 7 | 148 | 39504 | 12.5 | 0.78 | — |
| Down 25 | sp\|Q9UNN8 | PROCR | Endothelial protein C receptor | 103 | 27909 | 15.1 | 0.80 | — |
| Down 26 | sp\|Q86SF2 | GALNT7 | N-Acetylgalactosaminyltransferase 7 | 95 | 89410 | 9.9 | 0.81 | — |
| Down 27 | tr\|I3L0U2 | PRSS21 | Testisin (fragment) | 115 | 27083 | 14.7 | 0.82 | Secreted trypsin-like serine protease |
| Down 28 | tr\|B7ZLP5 | SAFB | SAFB protein | 557 | 121835 | 13 | 0.83 | — |
| Down 29 | tr\|F2Z3N7 | TMEM106B | Transmembrane protein 106B | 135 | 12975 | 12.5 | 0.82 | — |
| Down 30 | tr\|B7Z361 | — | Reticulon | 166 | 27838 | 12.2 | 0.76 | — |
| Down 31 | tr\|H0Y6F2 | PRR5 | Proline-rich protein 5 (fragment) | 57 | 39929 | 2.3 | 0.78 | — |
| Down 32 | sp\|Q7Z7E8 | UBE2Q1 | Ubiquitin-conjugating enzyme E2 Q1 | 92 | 54711 | 1.9 | 0.76 | — |
| Down 33 | tr\|A8K4K9 | — | cDNA FLJ76169 | 146 | 42007 | 8.8 | 0.83 | — |
| Down 34 | sp\|P13645 | KRT10 | Keratin, type I cytoskeletal 10 | 382 | 66321 | 21.6 | 0.55 | — |
| Down 35 | sp\|Q8N5K1 | CISD2 | CDGSH iron-sulfur domain-containing protein 2 | 167 | 20364 | 26.7 | 0.81 | — |
| Down 36 | sp\|Q8NI27 | THOC2 | THO complex subunit 2 | 282 | 241732 | 8.7 | 0.83 | — |
| Down 37 | tr\|B4DEP8 | — | cDNA FLJ56960, highly similar to Homo sapiens phosphatidylinositol 4-kinase type II (PI4KII), mRNA | 127 | 61711 | 9.8 | 0.76 | — |
| Down 38 | sp\|Q5BKZ1 | ZNF326 | DBIRD complex subunit ZNF326 | 145 | 78123 | 7.9 | 0.78 | — |
| Down 39 | tr\|Q8IW24 | EXOC5 | Exocyst complex component 5 | 108 | 99962 | 9.3 | 0.82 | — |
| Down 40 | tr\|B3KMG6 | — | cDNA FLJ10939 fis, clone OVARC1001065, highly similar to Homo sapiens MTERF domain containing 1 (MTERFD1), mRNA | 117 | 43225 | 9.8 | 0.76 | — |
| Down 41 | sp\|Q8NBM4-2 | UBAC2 | Isoform 2 of ubiquitin-associated domain-containing protein 2 | 150 | 37306 | 18.1 | 0.83 | — |
| Down 42 | sp\|Q8NGA1 | OR1M1 | Olfactory receptor 1M1 | 76 | 39512 | 2.2 | 0.69 | — |
| Down 43 | tr\|E9PN17 | ATP5L | ATP synthase subunit g, mitochondrial | 366 | 11489 | 63.2 | 0.82 | — |
| Down 44 | tr\|B2R686 | TGOLN2 | Trans-golgi network protein 2, isoform CRA_a | 166 | 61093 | 13 | 0.79 | — |
| Down 45 | tr\|B4DIR5 | — | cDNA FLJ56026 | 51 | 143728 | 1.7 | 0.74 | — |
| Down 46 | tr\|J3KS15 | ICT1 | Peptidyl-tRNA hydrolase ICT1, mitochondrial (fragment) | 169 | 26740 | 26 | 0.82 | Protein chain release factor B |
| Down 47 | tr\|F5H0F9 | ANAPC5 | Anaphase-promoting complex subunit 5 | 72 | 98300 | 7.5 | 0.82 | — |
| Down 48 | tr\|C8C504 | HBB | Beta-globin | 1233 | 20056 | 29.9 | 0.21 | — |
| Down 49 | tr\|B2R921 | — | cDNA, FLJ94171, highly similar to Homo sapiens solute carrier family 25 (mitochondrial carrier; ornithine transporter) member 15 (SLC25A15), nuclear gene encoding mitochondrial protein, mRNA | 53 | 39308 | 9 | 0.77 | — |
| Down 50 | sp\|Q9Y613 | FHOD1 | FH1/FH2 domain-containing protein 1 | 255 | 141625 | 8.8 | 0.81 | — |
| Down 51 | sp\|Q92643 | PIGK | GPI-anchor transamidase | 110 | 51592 | 10.9 | 0.77 | Glycosylphosphatidylinositol transamidase (GPIT), subunit GPI8 |
| Down 52 | tr\|A4FTY4 | TXNRD2 | TXNRD2 protein | 331 | 41672 | 24.6 | 0.79 | Pyruvate/2-oxoglutarate dehydrogenase complex, dihydrolipoamide dehydrogenase (E3) component, and related enzymes |

Table 2: Continued.

| Rank # | Accession | Gene symbol (GN) | Definition (description) | Score | Mass | Cov% | Ration | COG function-description |
|---|---|---|---|---|---|---|---|---|
| Down 53 | tr\|D3DP46 | SPCS3 | Signal peptidase complex subunit 3 homolog (*S. cerevisiae*), isoform CRA_a | 147 | 24007 | 18.9 | 0.82 | — |
| Down 54 | sp\|Q9Y5Q9 | GTF3C3 | General transcription factor 3C polypeptide 3 | 154 | 117216 | 7.8 | 0.79 | — |
| Down 55 | sp\|P60468 | SEC61B | Protein transport protein Sec61 subunit beta | 192 | 11546 | 37.5 | 0.72 | — |
| Down 56 | sp\|Q5RI15-2 | — | Isoform 2 of cytochrome c oxidase protein 20 homolog | 106 | 17682 | 20 | 0.83 | — |
| Down 57 | sp\|Q9P206-2 | — | Isoform 2 of uncharacterized protein KIAA1522 | 146 | 128602 | 6.5 | 0.73 | — |
| Down 58 | sp\|Q86YN1 | DOLPP1 | Dolichyldiphosphatase 1 | 64 | 28953 | 5.5 | 0.69 | Membrane-associated phospholipid phosphatase |
| Down 59 | sp\|O00165-2 | — | Isoform 2 of HCLS1-associated protein X-1 | 111 | 34281 | 16 | 0.81 | — |
| Down 60 | tr\|B4E303 | — | cDNA FLJ57449, highly similar to Notchless homolog 1 | 127 | 54134 | 16.5 | 0.82 | FOG: WD40 repeat |
| Down 61 | sp\|O00194 | RAB27B | Ras-related protein Rab-27B | 56 | 29688 | 14.2 | 0.77 | GTPase SAR1 and related small G proteins |
| Down 62 | tr\|B4DI41 | MBD1 | Methyl-CpG-binding domain protein 1 | 72 | 87409 | 1.8 | 0.80 | — |
| Down 63 | tr\|B0UXB6 | ABHD16A | Abhydrolase domain-containing protein 16A | 129 | 73275 | 10.3 | 0.83 | Hydrolases of the alpha/beta superfamily |
| Down 64 | sp\|Q5T8D3-2 | — | Isoform 2 of Acyl-CoA-binding domain-containing protein 5 | 148 | 64353 | 11.6 | 0.72 | Acyl-CoA-binding protein |
| Down 65 | tr\|B4DNZ6 | GTF2H3 | General transcription factor IIH subunit 3 | 48 | 37020 | 4.5 | 0.79 | RNA polymerase II transcription initiation/nucleotide excision repair factor TFIIH, subunit TFB4 |
| Down 66 | sp\|Q96FQ6 | S100A16 | Protein S100-A16 | 346 | 15197 | 22.3 | 0.83 | — |
| Down 67 | tr\|B4DSE1 | — | cDNA FLJ55364, highly similar to CRSP complex subunit 6 | 55 | 84524 | 3.7 | 0.73 | — |
| Down 68 | tr\|J3KNX9 | MYO18A | Unconventional myosin-XVIIIa | 157 | 282257 | 3.5 | 0.72 | Myosin heavy chain |
| Down 69 | tr\|B4DMK6 | — | cDNA FLJ60055, highly similar to *Rattus norvegicus* Ssu72 RNA polymerase II CTD phosphatase homolog, mRNA | 51 | 23745 | 13.5 | 0.82 | RNA polymerase II-interacting protein involved in transcription start site selection |
| Down 70 | tr\|G3V1A0 | TRAPPC4 | HCG38438, isoform CRA_b | 51 | 14838 | 20.5 | 0.81 | — |
| Down 71 | tr\|B1AHA8 | HMOX1 | Heme oxygenase 1 (fragment) | 53 | 25525 | 15.5 | 0.83 | Heme oxygenase |
| Down 72 | sp\|Q9Y3B3-2 | TMED7 | Isoform 2 of transmembrane emp24 domain-containing protein 7 | 193 | 24908 | 28.2 | 0.82 | — |
| Down 73 | tr\|G3V1U5 | GOLT1B | Golgi transport 1 homolog B (*S. cerevisiae*), isoform CRA_c | 167 | 9121 | 20.3 | 0.77 | Membrane protein involved in Golgi transport |
| Down 74 | tr\|B1PBA3 | — | SKNY protein | 148 | 109440 | 8.4 | 0.81 | — |
| Down 75 | sp\|Q15061 | WDR43 | WD repeat-containing protein 43 | 138 | 91327 | 5.6 | 0.83 | FOG: WD40 repeat |
| Down 76 | tr\|D3DUJ0 | AFG3L2 | AFG3 ATPase family gene 3-like 2 (yeast), isoform CRA_a (fragment) | 695 | 103842 | 21.2 | 0.83 | ATP-dependent Zn proteases |
| Down 77 | tr\|B2RBL9 | — | cDNA, FLJ95582, highly similar to Homo sapiens breast cancer antiestrogen resistance 1 (BCAR1), mRNA | 204 | 104223 | 6 | 0.79 | — |
| Down 78 | sp\|Q3SXM5-2 | — | Isoform 2 of inactive hydroxysteroid dehydrogenase-like protein 1 | 170 | 35499 | 13.5 | 0.83 | Short-chain dehydrogenases of various substrate specificities |

Table 2: Continued.

| Rank # | Accession | Gene symbol (GN) | Definition (description) | Score | Mass | Cov% | Ration | COG function-description |
|---|---|---|---|---|---|---|---|---|
| Down 79 | sp\|O43920 | NDUFS5 | NADH dehydrogenase [ubiquinone] iron-sulfur protein 5 | 106 | 16388 | 11.3 | 0.74 | — |
| Down 80 | tr\|H0YG20 | MAN1B1 | Endoplasmic reticulum mannosyl-oligosaccharide 1,2-alpha-mannosidase (fragment) | 155 | 90816 | 8.2 | 0.80 | — |
| Down 81 | tr\|Q0KKI6 | — | Immunoglobulin light chain (fragment) | 66 | 28559 | 8.2 | 0.80 | — |
| Down 82 | sp\|P62244 | RPS15A | 40S ribosomal protein S15a | 1521 | 18594 | 66.2 | 0.82 | Ribosomal protein S8 |
| Down 83 | tr\|B4DL07 | — | cDNA FLJ53353, highly similar to ATP-binding cassette subfamily D member 3 | 398 | 92669 | 16.7 | 0.81 | ABC-type uncharacterized transport system, permease, and ATPase components |
| Down 84 | tr\|B4DR67 | ALG5 | Dolichyl-phosphate beta-glucosyltransferase | 66 | 32213 | 10.9 | 0.81 | Glycosyltransferases involved in cell wall biogenesis |
| Down 85 | tr\|Q9BTT5 | — | Similar to NADH dehydrogenase (ubiquinone) 1 alpha subcomplex, 9 (39 kD) (fragment) | 189 | 45471 | 21 | 0.75 | Predicted nucleoside-diphosphate-sugar epimerases |
| Down 86 | tr\|Q5U0H8 | — | Myelin protein zero-like 1 | 55 | 34725 | 4.8 | 0.74 | — |
| Down 87 | sp\|Q5SY16 | NOL9 | Polynucleotide 5-hydroxyl-kinase NOL9 | 109 | 91782 | 7.4 | 0.79 | Predicted GTPase or GTP-binding protein |
| Down 88 | sp\|O15173-2 | PGRMC2 | Isoform 2 of membrane-associated progesterone receptor component 2 | 620 | 30166 | 26.3 | 0.75 | — |
| Down 89 | sp\|Q5VT52-3 | RPRD2 | Isoform 3 of regulation of nuclear pre-mRNA domain-containing protein 2 | 295 | 177879 | 4.5 | 0.82 | — |
| Down 90 | sp\|Q8TC12 | RDH11 | Retinol dehydrogenase 11 | 494 | 41238 | 14.5 | 0.76 | Dehydrogenases with different specificities (related to short-chain alcohol dehydrogenases) |
| Down 91 | tr\|B4DZ55 | — | cDNA FLJ52097, weakly similar to Homo sapiens transmembrane and tetratricopeptide repeat containing 1 (TMTC1), mRNA | 164 | 126875 | 10.1 | 0.79 | FOG: TPR repeat |
| Down 92 | tr\|J3KQA9 | MTUS2 | Microtubule-associated tumor suppressor candidate 2 | 150 | 181383 | 0.6 | 0.77 | — |
| Down 93 | sp\|Q96MG7 | NDNL2 | Melanoma-associated antigen G1 | 58 | 41645 | 7.6 | 0.72 | — |
| Down 94 | tr\|H3BQH3 | KLHDC4 | Kelch domain-containing protein 4 (fragment) | 107 | 47359 | 10.7 | 0.83 | — |
| Down 95 | tr\|J3KN00 | NDUFA13 | NADH dehydrogenase (ubiquinone) 1 alpha subcomplex, 13 | 258 | 28599 | 23.3 | 0.81 | — |
| Down 96 | sp\|Q8NF37 | LPCAT1 | Lysophosphatidylcholine acyltransferase 1 | 708 | 67346 | 15.7 | 0.82 | 1-Acyl-sn-glycerol-3-phosphate acyltransferase |
| Down 97 | sp\|Q9Y5P4-2 | COL4A3BP | Isoform 2 of collagen type IV alpha-3-binding protein | 82 | 81121 | 6.7 | 0.80 | — |
| Down 98 | tr\|Q5T8U5 | SURF4 | Surfeit 4 | 418 | 22863 | 39.8 | 0.81 | Predicted membrane protein |
| Down 99 | sp\|P26599-2 | PTBP1 | Isoform 2 of polypyrimidine tract-binding protein 1 | 570 | 69515 | 16.2 | 0.82 | — |
| Down 100 | sp\|Q8NC56 | LEMD2 | LEM domain-containing protein 2 | 137 | 63423 | 7.4 | 0.76 | — |
| Down 101 | tr\|Q2Q9H2 | G6PD | Glucose-6-phosphate 1-dehydrogenase (fragment) | 2165 | 64315 | 58.3 | 0.80 | Glucose-6-phosphate 1-dehydrogenase |
| Down 102 | sp\|P21796 | VDAC1 | Voltage-dependent anion-selective channel protein 1 | 2340 | 38777 | 62.9 | 0.80 | — |
| Down 103 | tr\|J3KNH7 | SENP3 | Sentrin-specific protease 3 | 88 | 73986 | 7.7 | 0.78 | Protease, Ulp1 family |

Table 2: Continued.

| Rank # | Accession | Gene symbol (GN) | Definition (description) | Score | Mass | Cov% | Ration | COG function-description |
|---|---|---|---|---|---|---|---|---|
| Down 104 | sp\|A6NHL2-2 | TUBAL3 | Isoform 2 of tubulin alpha chain-like 3 | 768 | 51287 | 11.8 | 0.79 | Tubulin |
| Down 105 | tr\|B4DR71 | — | cDNA FLJ57078, highly similar to Homo sapiens opioid receptor, sigma 1 (OPRS1), transcript variant 1, mRNA | 63 | 18151 | 8.4 | 0.83 | — |
| Down 106 | sp\|Q5JRA6-2 | MIA3 | Isoform 2 of melanoma inhibitory activity protein 3 | 415 | 249369 | 7.8 | 0.80 | — |
| Down 107 | tr\|J9ZVQ3 | APOE | Apolipoprotein E (fragment) | 171 | 30543 | 12.2 | 0.79 | — |
| Down 108 | tr\|G5E9V5 | MRPS22 | 28S ribosomal protein S22, mitochondrial | 224 | 49264 | 17.3 | 0.77 | — |
| Down 109 | tr\|B7Z7X8 | ATL2 | Atlastin-2 | 112 | 76668 | 10.8 | 0.82 | — |
| Down 110 | sp\|P54709 | ATP1B3 | Sodium/potassium-transporting ATPase subunit beta-3 | 243 | 39135 | 17.9 | 0.83 | — |
| Down 111 | tr\|Q6IBK3 | SCAMP2 | SCAMP2 protein | 258 | 39155 | 9.7 | 0.81 | — |
| Down 112 | tr\|A4LAA3 | ATRX | Alpha thalassemia/mental retardation syndrome X-linked | 129 | 374604 | 2.5 | 0.81 | Superfamily II DNA/RNA helicases, SNF2 family |
| Down 113 | sp\|Q9UK59 | DBR1 | Lariat debranching enzyme | 203 | 72182 | 14.5 | 0.80 | — |
| Down 114 | tr\|B4DI61 | — | cDNA FLJ58182, highly similar to protein CYR61 | 68 | 50414 | 6.4 | 0.70 | — |
| Down 115 | tr\|H3BNF1 | CLN6 | Ceroid-lipofuscinosis neuronal protein 6 | 300 | 12918 | 20 | 0.80 | — |
| Down 116 | tr\|E7ERK9 | EIF2B4 | Translation initiation factor eIF-2B subunit delta | 170 | 71199 | 8.8 | 0.79 | Translation initiation factor 2B subunit, eIF-2B alpha/beta/delta family |
| Down 117 | tr\|H0Y8C3 | MTCH1 | Mitochondrial carrier homolog 1 (fragment) | 97 | 50964 | 12.9 | 0.81 | — |
| Down 118 | tr\|B2RMV2 | CYTSA | CYTSA protein | 52 | 149539 | 2.5 | 0.79 | $Ca^{2+}$-binding actin-bundling protein fimbrin/plastin (EF-hand superfamily) |
| Down 119 | tr\|I3L1P8 | SLC25A11 | Mitochondrial 2-oxoglutarate/malate carrier protein (fragment) | 470 | 37200 | 35.5 | 0.83 | — |
| Down 120 | sp\|Q8NBU5-2 | ATAD1 | Isoform 2 of ATPase family AAA domain-containing protein 1 | 124 | 40468 | 11.1 | 0.72 | ATPases of the AAA+ class |
| Down 121 | sp\|Q9Y3E7 | CHMP3 | Charged multivesicular body protein 3 | 102 | 32415 | 14.4 | 0.83 | Conserved protein implicated in secretion |
| Down 122 | sp\|P02763 | ORM1 | Alpha-1-acid glycoprotein 1 | 262 | 28288 | 20.4 | 0.80 | — |
| Down 123 | tr\|Q53F51 | — | FGF intracellular binding protein isoform b variant (fragment) | 165 | 48798 | 12 | 0.83 | — |
| Down 124 | sp\|Q3ZAQ7 | VMA21 | Vacuolar ATPase assembly integral membrane protein VMA21 | 241 | 12868 | 24.8 | 0.81 | — |
| Down 125 | tr\|B2R6X8 | — | cDNA, FLJ93169, highly similar to Homo sapiens GPAA1P anchor attachment protein 1 homolog (yeast) (GPAA1), mRNA | 106 | 72151 | 7.6 | 0.80 | — |
| Down 126 | sp\|Q9P0S9 | TMEM14C | Transmembrane protein 14C | 45 | 12774 | 8.9 | 0.70 | — |
| Down 127 | sp\|P08779 | KRT16 | Keratin, type I cytoskeletal 16 | 630 | 57054 | 23.9 | 0.62 | — |
| Down 128 | sp\|Q86UT6-2 | NLRX1 | Isoform 2 of NLR family member X1 | 75 | 110309 | 4.1 | 0.71 | — |
| Down 129 | tr\|Q59E99 | — | Thrombospondin 1 variant (fragment) | 153 | 155789 | 3.4 | 0.68 | — |
| Down 130 | sp\|Q8WXH0-2 | SYNE2 | Isoform 2 of nesprin-2 | 149 | 986758 | 1.1 | 0.82 | $Ca^{2+}$-binding actin-bundling protein fimbrin/plastin (EF-hand superfamily) |

Table 2: Continued.

| Rank # | Accession | Gene symbol (GN) | Definition (description) | Score | Mass | Cov% | Ration | COG function-description |
|---|---|---|---|---|---|---|---|---|
| Down 131 | sp\|P78310-2 | CXADR | Isoform 2 of coxsackievirus and adenovirus receptor | 47 | 47491 | 3.8 | 0.74 | — |
| Down 132 | tr\|B2R995 | — | Malic enzyme | 98 | 77738 | 5.8 | 0.83 | Malic enzyme |
| Down 133 | tr\|Q5QP56 | BCL2L1 | Bcl-2-like protein 1 (fragment) | 98 | 21810 | 23.2 | 0.82 | — |
| Down 134 | tr\|H0YK72 | SEC11A | SEC11-like 1 (*S. cerevisiae*), isoform CRA_a | 247 | 22018 | 16.5 | 0.81 | Signal peptidase I |
| Down 135 | tr\|B4DDH8 | — | cDNA FLJ55184, highly similar to Homo sapiens leukocyte receptor cluster (LRC) member 4 (LENG4), mRNA | 137 | 54865 | 8.8 | 0.79 | Predicted membrane protein |
| Down 136 | sp\|Q9UJS0-2 | SLC25A13 | Isoform 2 of calcium-binding mitochondrial carrier protein Aralar2 | 719 | 86824 | 17.5 | 0.82 | — |
| Down 137 | tr\|A8KAK5 | — | cDNA FLJ77399, highly similar to Homo sapiens cofactor required for Sp1 transcriptional activation, subunit 2, 150 kDa (CRSP2), mRNA | 85 | 182987 | 3.4 | 0.82 | — |
| Down 138 | tr\|H0YEF3 | RNASEH2C | Ribonuclease H2 subunit C (fragment) | 76 | 18856 | 25.3 | 0.77 | — |
| Down 139 | tr\|Q5QNZ2 | ATP5F1 | ATP synthase F(0) complex subunit B1, mitochondrial | 406 | 27794 | 47.7 | 0.82 | — |
| Down 140 | sp\|Q6UW68 | TMEM205 | Transmembrane protein 205 | 165 | 23294 | 15.9 | 0.82 | — |
| Down 141 | tr\|B3KPJ4 | PHC2 | Polyhomeotic-like protein 2 | 193 | 59764 | 9.3 | 0.79 | — |
| Down 142 | tr\|H0Y4D4 | ACAA1 | 3-Ketoacyl-CoA thiolase, peroxisomal (fragment) | 131 | 30218 | 12.7 | 0.78 | Acetyl-CoA acetyltransferase |
| Down 143 | tr\|Q4G0F4 | POLRMT | DNA-directed RNA polymerase | 167 | 159664 | 4.6 | 0.81 | Mitochondrial DNA-directed RNA polymerase |
| Down 144 | tr\|Q6FGZ3 | EPHX1 | EPHX1 protein (fragment) | 519 | 62281 | 14.9 | 0.77 | Predicted hydrolases or acyltransferases (alpha/beta hydrolase superfamily) |
| Down 145 | tr\|B4DVN1 | — | cDNA FLJ52214, highly similar to DnaJ homolog subfamily B member 6 | 90 | 37740 | 8.6 | 0.70 | DnaJ-class molecular chaperone with C-terminal Zn finger domain |
| Down 146 | sp\|Q92667-2 | AKAP1 | A-kinase anchor protein 1, mitochondrial | 66 | 111940 | 4.9 | | |
| Down 147 | sp\|O00483 | NDUFA4 | NADH dehydrogenase [ubiquinone] 1 alpha subcomplex subunit 4 | 165 | 11855 | 46.9 | 0.83 | — |
| Down 148 | sp\|Q9NTJ5 | SACM1L | Phosphatidylinositide phosphatase SAC1 | 179 | 77476 | 18.2 | 0.83 | Phosphoinositide polyphosphatase (Sac family) |
| Down 149 | tr\|B3KVC5 | — | cDNA FLJ16380 fis, clone TLIVE2002882, weakly similar to imidazolonepropionase (EC 3.5.2.7) | 41 | 53582 | 3.3 | 0.83 | Imidazolonepropionase and related amidohydrolases |
| Down 150 | tr\|B7ZLI5 | FAM98C | Family with sequence similarity 98, member C | 72 | 41696 | 9.5 | 0.68 | — |
| Down 151 | tr\|B7Z6F5 | YIPF1 | Protein YIPF1 | 64 | 40866 | 2.7 | 0.61 | — |
| Down 152 | sp\|Q6NVY1-2 | HIBCH | Isoform 2 of 3-hydroxyisobutyryl-CoA hydrolase, mitochondrial | 101 | 46543 | 19.2 | 0.82 | Enoyl-CoA hydratase/carnitine racemase |
| Down 153 | tr\|U3KQJ1 | POLDIP2 | Polymerase delta-interacting protein 2 | 282 | 46395 | 26.4 | 0.76 | Uncharacterized protein affecting $Mg^{2+}/Co^{2+}$ transport |
| Down 154 | tr\|D6RGZ2 | THOC3 | THO complex subunit 3 | 172 | 12690 | 36.2 | 0.75 | — |
| Down 155 | tr\|A0S0T0 | ATP6 | ATP synthase subunit a | 128 | 26896 | 4.4 | 0.78 | F0F1-type ATP synthase, subunit a |
| Down 156 | tr\|G3V2U7 | ACYP1 | Acylphosphatase | 85 | 17520 | 14.7 | 0.80 | acylphosphatases |
| Down 157 | sp\|Q9ULG6-2 | CCPG1 | Isoform 2 of cell cycle progression protein 1 | 79 | 93313 | 4.1 | 0.81 | — |

Table 2: Continued.

| Rank # | Accession | Gene symbol (GN) | Definition (description) | Score | Mass | Cov% | Ration | COG function-description |
|---|---|---|---|---|---|---|---|---|
| Down 158 | tr\|H7BXZ6 | RHOT1 | Mitochondrial Rho GTPase | 142 | 81600 | 5.9 | 0.77 | GTPase SAR1 and related small G proteins |
| Down 159 | sp\|Q14151 | SAFB2 | Scaffold attachment factor B2 | 461 | 129824 | 13 | 0.83 | — |
| Down 160 | sp\|Q96LD4 | TRIM47 | Tripartite motif-containing protein 47 | 138 | 75838 | 7.8 | 0.81 | — |
| Down 161 | tr\|A8K2K2 | — | cDNA FLJ76494, highly similar to Homo sapiens GTPBP2 GTP-binding like protein 2 | 137 | 64767 | 11.7 | 0.83 | GTPase |

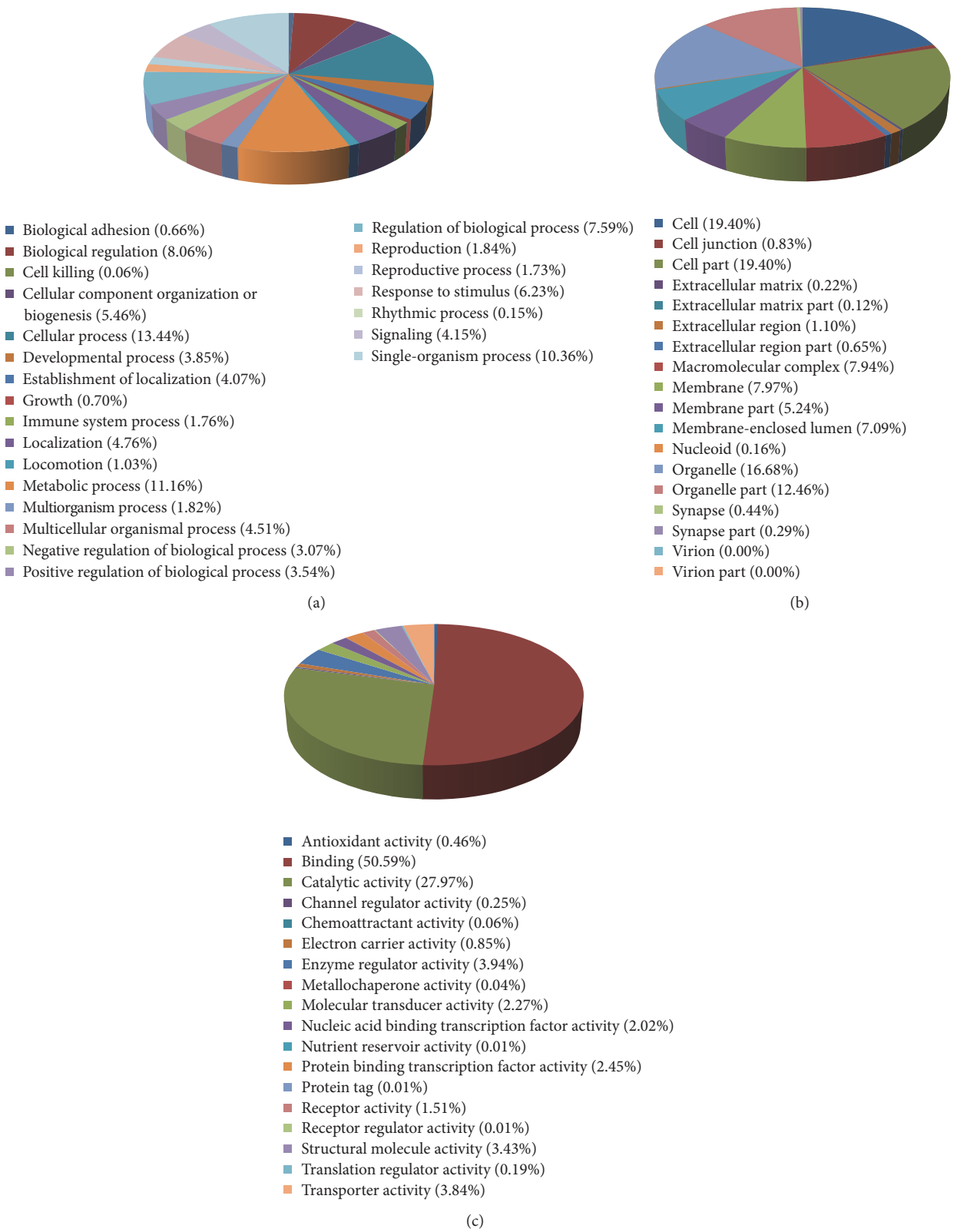


Figure 2: Classification of identified proteins. (a) The biological processes (BPs), (b) cellular components (CCs), and (c) molecular functions (MFs) of the total identified proteins classified by GO database.

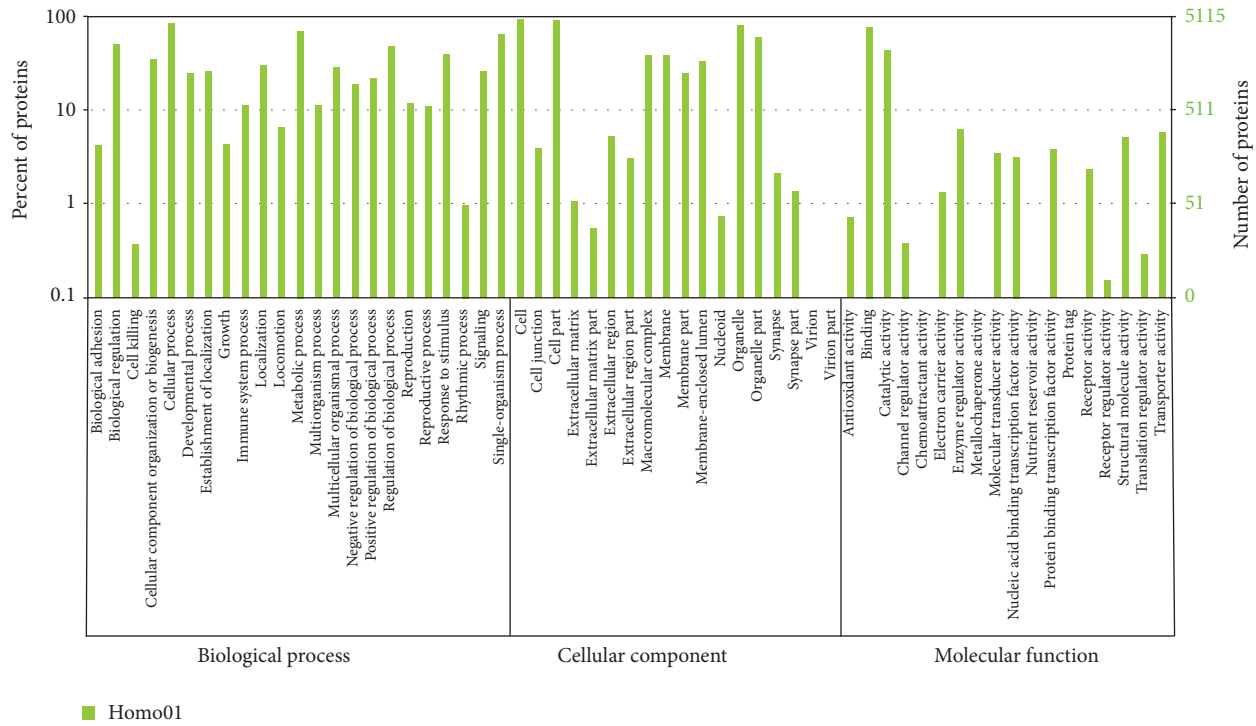


(a)

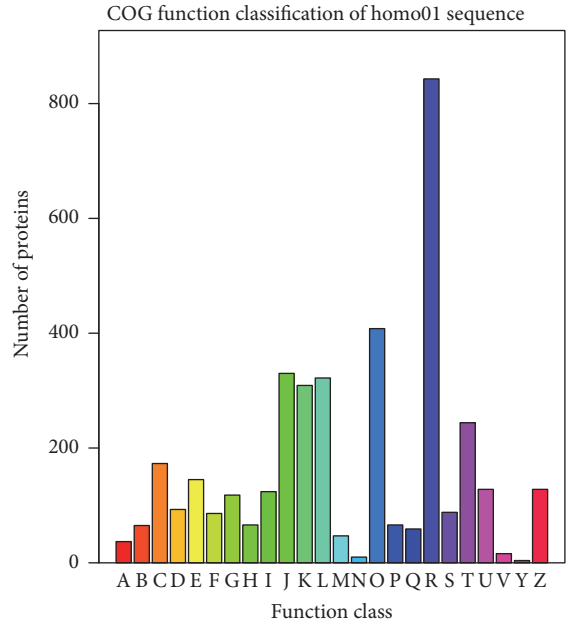


A: RNA processing and modification
B: chromatin structure and dynamics
C: energy production and conversion
D: cell cycle control, cell division, and chromosome partitioning
E: amino acid transport and metabolism
F: nucleotide transport and metabolism
G: carbohydrate transport and metabolism
H: coenzyme transport and metabolism
I: lipid transport and metabolism
J: translation, ribosomal structure, and biogenesis
K: transcription
L: replication, recombination, and repair
M: cell wall/membrane/envelope biogenesis
N: cell motility
O: posttranslational modification, and protein turnover, chaperones
P: inorganic ion transport and metabolism
Q: secondary metabolites biosynthesis, transport and catabolism
R: general function prediction only
S: function unknown
T: signal transduction mechanisms
U: intracellular trafficking, secretion, and vesicular transport
V: defense mechanisms
Y: nuclear structure
Z: cytoskeleton

(b)

Figure 3: WEGO (a) and COG (b) assay of the 205 differentially expressed proteins.

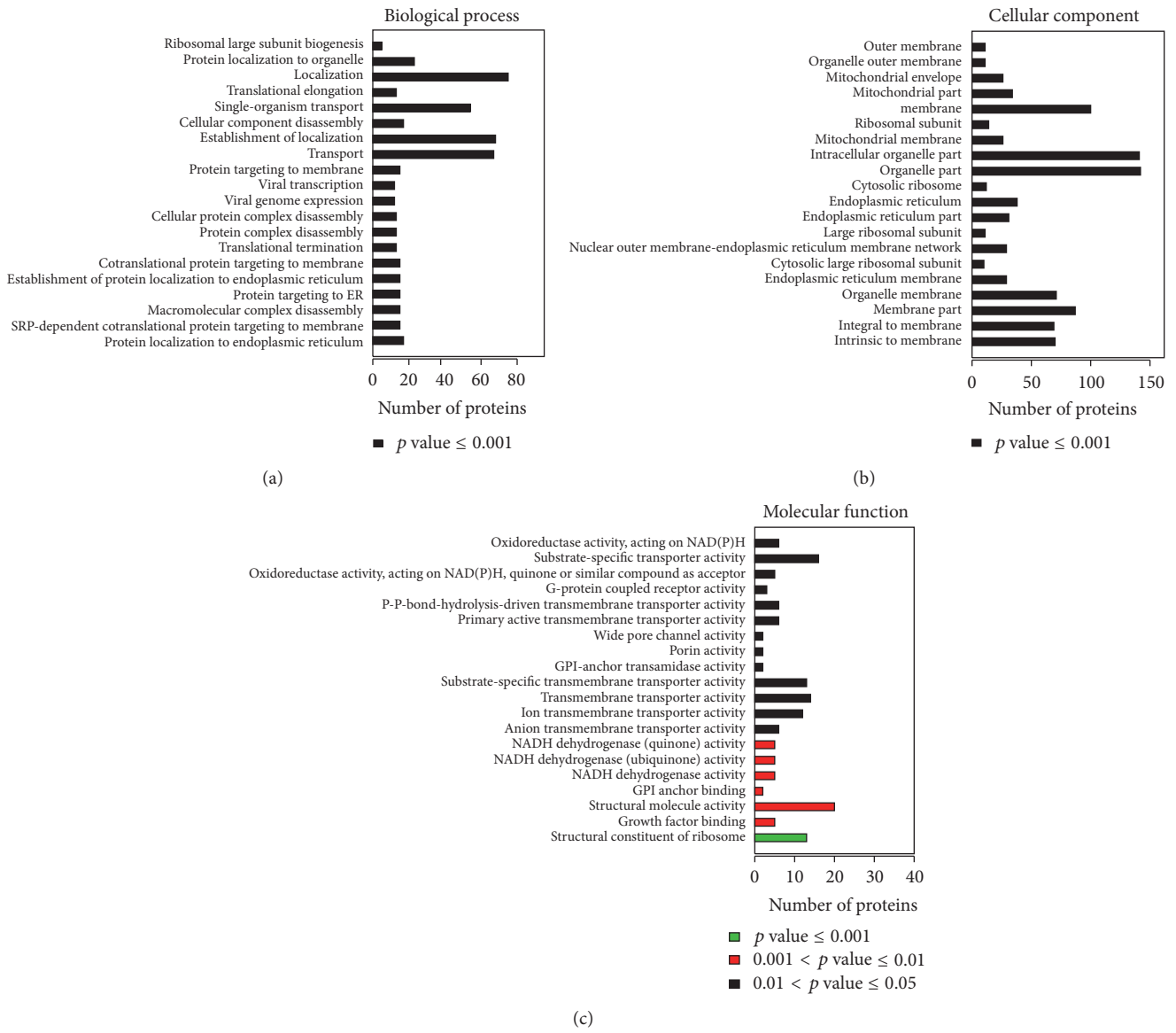


Figure 4: GO annotation of the final selected differentially expressed proteins. The top 20 components for BP (a), CC (b), and MF (c) of the selected differentially expressed proteins are shown along with their enrichment score, represented as a $p$ value.

differentially expressed proteins were identified with ≥95% confidence in ginsenoside $F_2$ treated group. Application of a ratio of 1.2-fold change as criteria resulted in 44 and 161 differentially abundant proteins in SGC7901 cells.

In our study, some proteins that were significantly altered by ginsenoside $F_2$ show close relationship of protein-protein interaction (Figure 5). Ribosomal proteins, such as RPS15 and RPL26, exert critical roles in MDM2-p53 signal pathway [11, 12]. PRR5 [13], CISD2 [14], Bcl-xl [15], and NLRX1 [16, 17] have been reported to play a key role in the regulation of autophagy or apoptosis. The changes of these six potential proteins were verified by western blot analysis.

Ribosomal proteins (RPs) are considered to have diverse extra ribosomal functions, ranging from cell cycle progression to cell death and to malignant transformation and cellular metabolism [11]. Relevantly, a number of RPs have been shown to bind to MDM2, the inhibitor of p53 (murine double minute 2, and also HDM2 for its human ortholog), and inhibit MDM2 E3 ligase activity, leading to p53 stabilization and activation, then triggering apoptosis or autophagy [11]. Following the treatment of ginsenoside $F_2$ in SGC7901 cells, the levels of RPL28, RPL34, RPL35, RPS16, RPL17, RPL14, RPL24, RPL7A, and RPL26 were increased, whereas that of RPS15 reduced. Although the functions of RPL28, RPL34, RPL35, RPS16, RPL17, RPL14, RPL24, and RPL7A have not been well studied, RPL26, a positive regulator of p53, was found to increase the translational rate of p53 mRNA by binding to its 50 untranslated region [12] and, in this case, MDM2 acts as an ubiquitin E3 ligase for ubiquitylation and degradation of RPL26 [18]. Thus, under the treatment of ginsenoside $F_2$, the increased level of RPL26 indicated that RPL26 may inhibit MDM2 and subsequently activate p53.

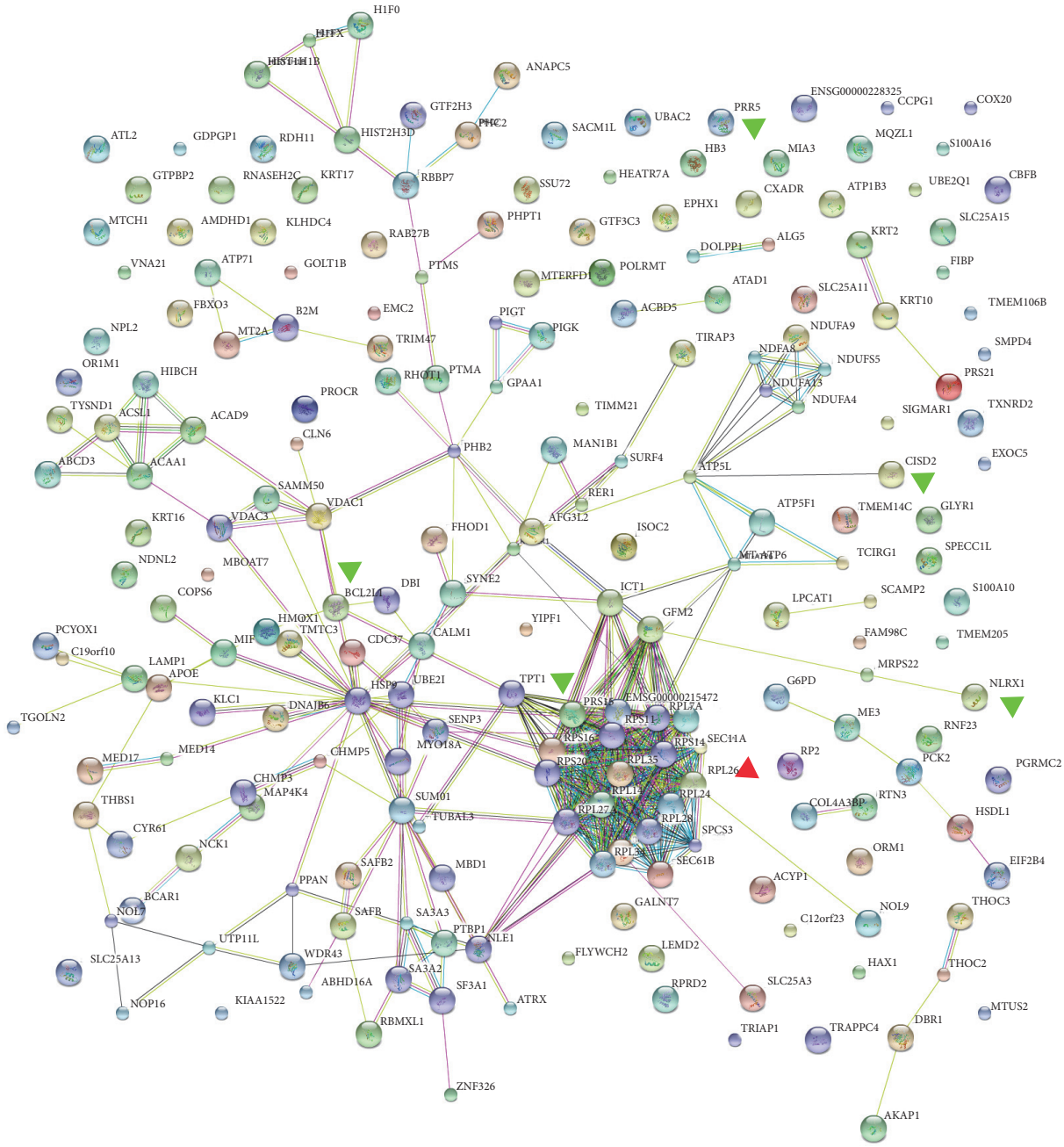


FIGURE 5: The protein-protein interaction network of the differentially expressed proteins identified. Red triangle denotes upregulated proteins; green triangle denotes downregulated protein.

RPS15, identified as a direct p53 transcriptional target, was thought to activate p53 by repressing MDM2 activity [19]. Interestingly, in our study, the level of RPS15 reduced in SGC7901 followed by ginsenoside $F_2$ treatment, suggesting that the roles of RPS15 and RPL26 involved in the anticancer mechanism of ginsenoside $F_2$ are different, which warrant further investigation.

mTOR, existing in two multiprotein complexes, mTORC1 and mTORC2, regulates cell growth in response to a variety of cellular signals derived from growth factors and environmental stress [20]. mTORC2 is a kinase complex comprised of mTOR, PRR5, Rictor, mSin1, and mLST8/GbL. The expression level of PRR5 is correlated with that of mTORC2. Recent study showed that mTORC2 is implicated

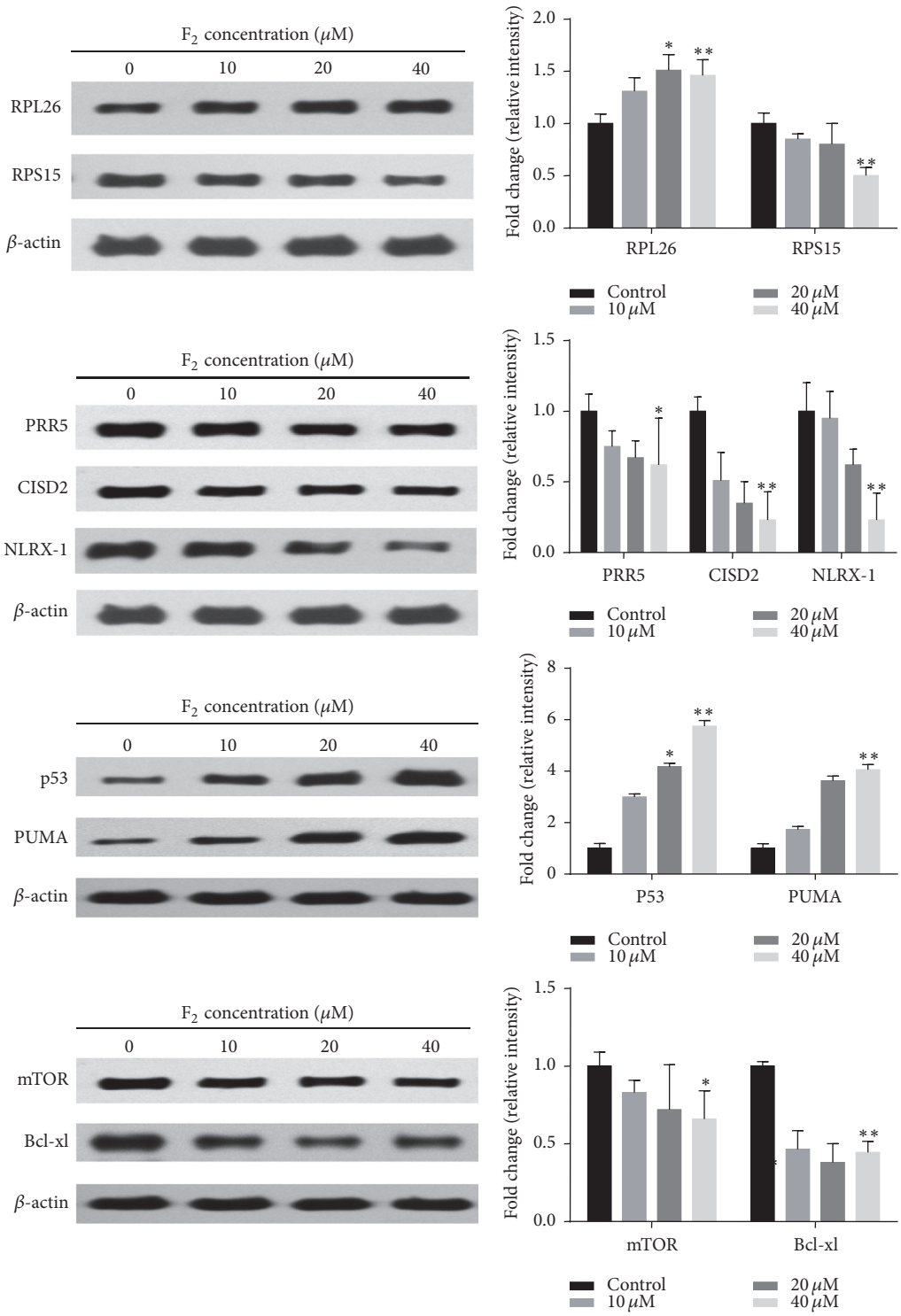


Figure 6: Western blot validations of RPS15, RPL26, PRR5, CISD2, NLRX1, p53, PUMA, mTOR, and Bcl-xl in SGC7901 cells with different concentrations of ginsenoside $F_2$. $1 \times 10^6$ SGC7901 cells are seeded in 6-well plate for overnight. On day 2, the cultured cells are treated with different concentration ginsenoside $F_2$. 12 hours after treatment, the protein is prepared by lysating cells with RIPA buffer for performing western blot analysis. Left panel: the representative western blot analysis. $\beta$-actin was used as the loading control. Right panel: accumulated results show the relative protein density. Error bars represent means ± SEMs. Significant difference is expressed as $^{**}p < 0.01$, $^{*}p < 0.05$.

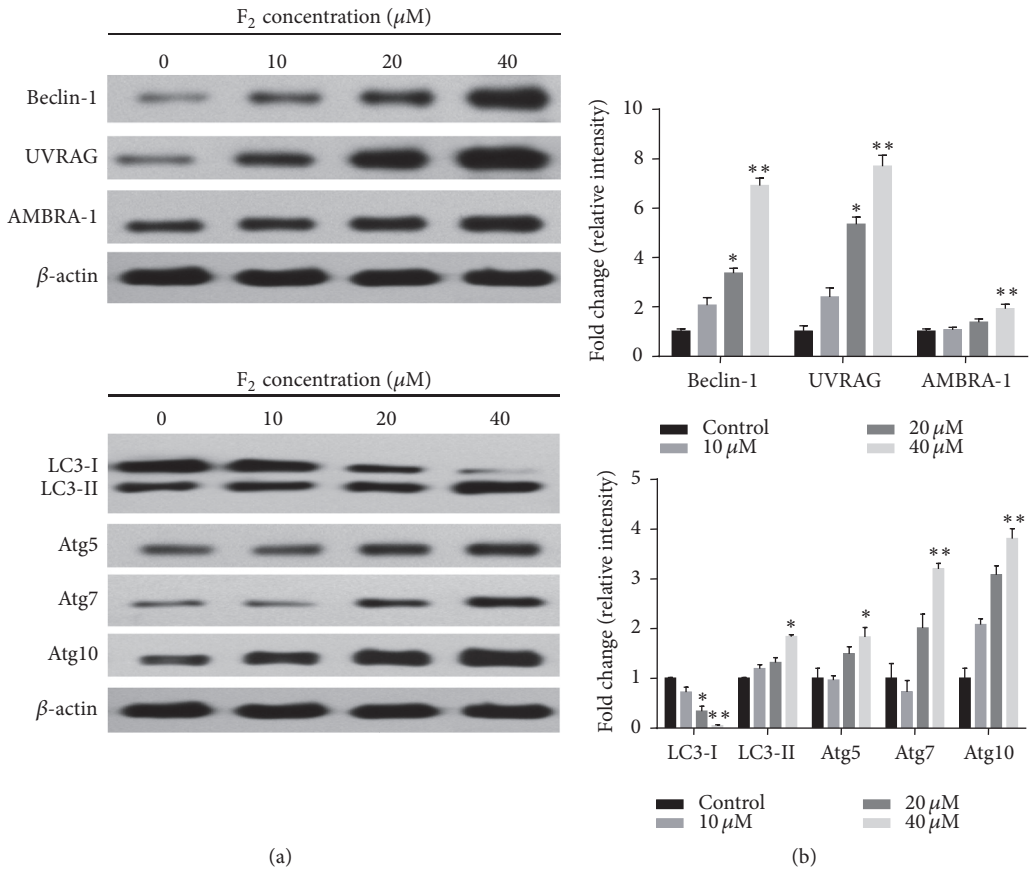


Figure 7: Effect of ginsenoside $F_2$ on the expression of Beclin-1, UVRAG, AMBRA-1, Atg5, Atg7, Atg10, LC3 I, and LC3-II. $1 \times 10^6$ SGC7901 cells are seeded in 6-well plate for overnight. On day 2, the cultured cells are treated with different concentration ginsenoside $F_2$. 12 hours after treatment, the protein is prepared by lysating cells with RIPA buffer for performing western blot analysis. Left panel: the representative western blot analysis. $\beta$-actin was used as the loading control. Right panel: accumulated results show the relative protein density. Error bars represent means ± SEMs. Significant difference is expressed as $^{**}p < 0.01$, $^{*}p < 0.05$.

in actin cytoskeleton regulation, as well as phosphorylation of Akt [13]. Although TOR kinase has been largely attributed as a negative regulator of autophagy through TORC1, resent study indicated that mTORC2 was an independent positive regulator of autophagy during amino acid starvation [21]. In the present study, ginsenoside $F_2$ decreased level of PPR5, indicated that ginsenoside $F_2$ may inhibit the expression of PRR5, and consequently inhibited mTORC2.

Recent study indicated that p53 can be a positive or negative regulator of autophagy. In the nucleus, p53 may activate the AMPK pathway and inhibit the mTOR pathway, subsequently triggering autophagy. p53 may also transactivate multiple genes with proautophagic roles, including proapoptotic Bcl-2 proteins (Bax, PUMA) [22, 23]. In this network, PUMA induces the noncanonical autophagy pathway regulated via Atg5, Atg7, and Atg10. PUMA's initiation of autophagy promotes cytochrome c release, which then leads to apoptosis [22]. Interestingly, in our previous work, increasing level of cytochrome c and decreased mitochondrial transmembrane potential (MTP) were observed [6]. In present study, decreased expressions of PRR5 and RPL26 were found, which implied that ginsenoside $F_2$ might trigger p53 signal pathway. It was reported that western blot analyses tended to show greater differential abundance compared with iTRAQ analyses [24]. Thus, the expressions of p53, Atg5, Atg7, Atg10, and PUMA were validated by western blot analyses. The increased level of Atg5 Atg7, Atg10, and PUMA and reduced level of P53 and mTORC2 suggested that ginsenoside $F_2$ may initiate autophagy by ribosomal protein-p53 signaling pathway.

CISD2, also known as NAF-1, Miner1, Eris, and Noxp70, is a member of the 2Fe-2S cluster NEET family [25]. Our results showed that CISD2 was significantly decreased in ginsenoside $F_2$ treated group, confirmed by western blot analysis. Recent work identified CISD2 as a Bcl-xl binding partner at a branch point between autophagy and apoptosis, life and death, under nutrient-deprived and oxidative stress conditions *in vivo* cells [25, 26]. Bcl-xl, also called Bcl-2L, is known to function through inhibition of the autophagy effector and tumor suppressor Beclin-1 [15]. CISD2 is required in this pathway for Bcl-xl to functionally antagonize Beclin-1-dependent autophagy. In our study, the expression of Bcl-xl decreased, confirmed by western blot analysis. Thus, CISD2 may be a Bcl-xl-associated cofactor that targets Bcl-2 for the autophagy pathway.

During initiation of autophagosome formation, after release from Bcl-xl, Beclin-1 functions as a platform by binding to class III PI3K/vacuolar protein sorting-34 (Vps34), UV-resistance-associated gene (UVRAG), activating molecule in Beclin-1-regulated autophagy (AMBRA-1) [15, 26, 27]. Previous studies have shown that binding of Beclin-1 to Bcl-2/Bcl-xl inhibits the autophagic function of Beclin-1, suggesting that Beclin-1 might have a role in the convergence between autophagy and apoptotic cell death [22]. For confirming the Beclin-1/Bcl-xl pathway, western blot was employed. The expressions of Beclin-1, UVRAG, and AMBRA-1 were increased, while Bcl-xl was decreased, which suggested that ginsenoside $F_2$ may induce autophagy via Bcl-xl/Beclin-1 pathway.

NLRX1, a mitochondrial NOD-like receptor that amplifies apoptosis by inducing reactive oxygen species production, is an important component of TLR mediated inflammatory pathways [13, 16]. Recent evidence suggested that upregulated expression of NLRX1 may synergistically regulate metabolism and autophagy for highly invasive growth of the autophagy addicted MDA-MB-231 breast cancer cells [16]. And it acted as tumor suppressor by regulating TNF-$\alpha$ induced apoptosis and metabolism in cancer cells. In our iTRAQ results, expression of NLRX1 was significantly decreased in SGC7901 cells treated with ginsenoside $F_2$. The phenomenon suggested different role of NLRX1 involved in the ginsenoside $F_2$ treatment that may be different from that of published reports [16, 17], though the mechanism needs further research.

Mai et al. reported that $F_2$ induces apoptotic cell death accompanied by protective autophagy in breast cancer stem cells [28]. In one of our previous studies, we found that $F_2$ induces apoptosis by causing an accumulation of ROS and activating the apoptosis signaling pathway [6]. However, there was no report systemically comparing differently regulated proteins and building a network of $F_2$-treated cancer cells at proteome level. In the current study, by the close look at cellular mechanisms at proteome level, we clearly identified the distinct pattern of cellular responses for the $F_2$-treated cells, and 6 differentially regulated proteins were identified, which provide useful information on elucidating the anticancer mechanism of $F_2$ to SGC7901 cells. Moreover, the integration of networks and pathway with the proteomic data enhanced our understanding of the functional relationship of proteome changes caused by the compound.

## 4. Conclusions

In conclusion, 44 upregulated proteins and 161 downregulated proteins were discovered by iTRAQ analysis in SGC7901 cells treated with lower dose and shorter duration of ginsenoside $F_2$, compared with our previous study. 6 differentially abundant common proteins, PRR5, CISD2, Bcl-xl, NLRX1, RPS15, and RPL26, were confirmed by western blot analysis. Ribosomal protein-p53 signaling pathway and Bcl-xl/Beclin-1 pathway might be significantly regulated biological process by ginsenoside $F_2$ treatment in SGC7901 cells. Although more work is required to find out the precise role of targeted proteins, our data lead to a better understanding of the molecular mechanisms of ginsenoside $F_2$ for gastric cancer treatment.

## Abbreviations

| | |
|---|---|
| iTRAQ: | Isobaric tag for relative and absolute quantification |
| KEGG: | Kyoto Encyclopedia of Genes and Genomes |
| COG: | Cluster of orthologous groups of proteins |
| Go: | Gene Ontology |
| FBS: | Fetal bovine serum |
| SCX: | Strong cation exchange |
| HCD: | High-energy collision dissociation |
| AGC: | Automatic gain control |
| NR: | Nonredundant protein database |
| SDS-PAGE: | Sodium dodecyl sulfate polyacrylamide gel electrophoresis |
| ECL: | Enhanced chemiluminescence |
| BP: | Biological process |
| CC: | Cellular component |
| MF: | Molecular function |
| RPs: | Ribosomal proteins |
| MTP: | Mitochondrial transmembrane potential |
| Vps34: | Vacuolar protein sorting-34 |
| UVRAG: | UV-resistance-associated gene |
| AMBRA-1: | Activating molecule in Beclin-1-regulated autophagy. |

## Competing Interests

The authors declare that there is no conflict of interests.

## Acknowledgments

This work was supported by the Natural Science Foundation of China (nos. 81573596, 81503191, 81274018, 81373946, and 81303221) and National High Technology Research and Development Plan of China (863 Plan) (2014AA022204).

## References

[1] E. Van Cutsem, X. Sagaert, B. Topal et al., "Gastric cancer," *The Lancet*, 2016.

[2] E. Niccolai, A. Taddei, D. Prisco, and A. Amedei, "Gastric cancer and the epoch of immunotherapy approaches," *World Journal of Gastroenterology*, vol. 21, no. 19, pp. 5778–5793, 2015.

[3] P. van Hagen, M. C. C. M. Hulshof, J. J. B. van Lanschot et al., "Preoperative chemoradiotherapy for esophageal or junctional cancer," *The New England Journal of Medicine*, vol. 366, no. 22, pp. 2074–2084, 2012.

[4] S. Chen, Z. Wang, Y. Huang et al., "Ginseng and anticancer drug combination to improve cancer chemotherapy: a critical review," *Evidence-Based Complementary and Alternative Medicine*, vol. 2014, Article ID 168940, 13 pages, 2014.

[5] L.-W. Qi, C.-Z. Wang, and C.-S. Yuan, "American ginseng: potential structure-function relationship in cancer chemoprevention," *Biochemical Pharmacology*, vol. 80, no. 7, pp. 947–954, 2010.

[6] Q. Mao, P.-H. Zhang, Q. Wang, and S.-L. Li, "Ginsenoside $F_2$ induces apoptosis in humor gastric carcinoma cells through reactive oxygen species-mitochondria pathway and modulation of ASK-1/JNK signaling cascade *in vitro* and *in vivo*," *Phytomedicine*, vol. 21, no. 4, pp. 515–522, 2014.

[7] J.-Y. Shin, J.-M. Lee, H.-S. Shin et al., "Anti-cancer effect of ginsenoside $F_2$ against glioblastoma multiforme in xenograft model in SD rats," *Journal of Ginseng Research*, vol. 36, no. 1, pp. 86–92, 2012.

[8] W. Cao, Y. Zhou, Y. Li et al., "iTRAQ-based proteomic analysis of combination therapy with taurine, epigallocatechin gallate, and genistein on carbon tetrachloride-induced liver fibrosis in rats," *Toxicology Letters*, vol. 232, no. 1, pp. 233–245, 2015.

[9] D. Dou, Y. Wen, M. Weng et al., "Minor saponins from leaves of *Panax ginseng* C.A. Meyer," *Zhongguo Zhong Yao Za Zhi*, vol. 22, no. 1, pp. 35–37, 1997.

[10] X. Hu, W. Han, and L. Li, "Targeting the weak point of cancer by induction of necroptosis," *Autophagy*, vol. 3, no. 5, pp. 490–492, 2007.

[11] W. Wang, S. Nag, X. Zhang et al., "Ribosomal proteins and human diseases: pathogenesis, molecular mechanisms, and therapeutic implications," *Medicinal Research Reviews*, vol. 35, no. 2, pp. 225–285, 2015.

[12] M. Takagi, M. J. Absalon, K. G. McLure, and M. B. Kastan, "Regulation of p53 translation and induction after DNA damage by ribosomal protein L26 and nucleolin," *Cell*, vol. 123, no. 1, pp. 49–63, 2005.

[13] S.-Y. Woo, D.-H. Kim, C.-B. Jun et al., "PRR5, a novel component of mTOR complex 2, regulates platelet-derived growth factor receptor $\beta$ expression and signaling," *The Journal of Biological Chemistry*, vol. 282, no. 35, pp. 25604–25612, 2007.

[14] N. C. Chang, M. Nguyen, M. Germain, and G. C. Shore, "Antagonism of Beclin 1-dependent autophagy by BCL-2 at the endoplasmic reticulum requires NAF-1," *The EMBO Journal*, vol. 29, no. 3, pp. 606–618, 2010.

[15] S.-Y. Kim, X. Song, L. Zhang, D. L. Bartlett, and Y. J. Lee, "Role of Bcl-xL/Beclin-1 in interplay between apoptosis and autophagy in oxaliplatin and bortezomib-induced cell death," *Biochemical Pharmacology*, vol. 88, no. 2, pp. 178–188, 2014.

[16] I. Tattoli, L. A. Carneiro, M. Jéhanno et al., "NLRX1 is a mitochondrial NOD-like receptor that amplifies NF-$\kappa$B and JNK pathways by inducing reactive oxygen species production," *EMBO Reports*, vol. 9, no. 3, pp. 293–300, 2008.

[17] X. Xia, J. Cui, H. Y. Wang et al., "NLRX1 negatively regulates TLR-induced NF-$\kappa$B signaling by targeting TRAF6 and IKK," *Immunity*, vol. 34, no. 6, pp. 843–853, 2011.

[18] Y. Ofir-Rosenfeld, K. Boggs, D. Michael, M. B. Kastan, and M. Oren, "Mdm2 regulates p53 mRNA translation through inhibitory interactions with ribosomal protein L26," *Molecular Cell*, vol. 32, no. 2, pp. 180–189, 2008.

[19] L. Daftuar, Y. Zhu, X. Jacq, and C. Prives, "Ribosomal proteins RPL37, RPS15 and RPS20 regulate the Mdm2-p53-MdmX network," *PLoS ONE*, vol. 8, no. 7, Article ID e68667, 2013.

[20] S. C. Johnson, P. S. Rabinovitch, and M. Kaeberlein, "mTOR is a key modulator of ageing and age-related disease," *Nature*, vol. 493, no. 7432, pp. 338–345, 2013.

[21] A. Vlahakis and T. Powers, "A role for TOR complex 2 signaling in promoting autophagy," *Autophagy*, vol. 10, no. 11, pp. 2085–2086, 2014.

[22] J. J. Tang, J. H. Di, H. Cao, J. Bai, and J. Zheng, "p53-Mediated autophagic regulation: a prospective strategy for cancer therapy," *Cancer Letters*, vol. 363, no. 2, pp. 101–107, 2015.

[23] R. Mathew, V. K. Wadsworth, and E. White, "Role of autophagy in cancer," *Nature Reviews Cancer*, vol. 7, no. 12, pp. 961–967, 2007.

[24] R. Ralhan, L. V. Desouza, A. Matta et al., "iTRAQ-multidimensional liquid chromatography and tandem mass spectrometry-based identification of potential biomarkers of oral epithelial dysplasia and novel networks between inflammation and premalignancy," *Journal of Proteome Research*, vol. 8, no. 1, pp. 300–309, 2009.

[25] S. Tamir, S. Rotem-Bamberger, C. Katz et al., "Integrated strategy reveals the protein interface between cancer targets Bcl-2 and NAF-1," *Proceedings of the National Academy of Sciences of the United States of America*, vol. 111, no. 14, pp. 5177–5182, 2014.

[26] G. M. Fimia, A. Stoykova, A. Romagnoli et al., "Ambra1 regulates autophagy and development of the nervous system," *Nature*, vol. 447, no. 7148, pp. 1121–1125, 2007.

[27] C. Liang, P. Feng, B. Ku et al., "Autophagic and tumour suppressor activity of a novel Beclin1-binding protein UVRAG," *Nature Cell Biology*, vol. 8, no. 7, pp. 688–698, 2006.

[28] T. T. Mai, J. Y. Moon, Y. W. Song et al., "Ginsenoside $F_2$ induces apoptosis accompanied by protective autophagy in breast cancer stem cells," *Cancer Letters*, vol. 321, no. 2, pp. 144–153, 2012.